Article

Synthesis of Crystalline Skutterudite Superlattices Using the Modulated Elemental Reactant Method

Joshua R. Williams, Arwyn L. E. Smalley, Heike Sellinschegg, Carrie Daniels-Hafer, Jennifer Harris, Mark B. Johnson, and David C. Johnson

J. Am. Chem. Soc., **2003**, 125 (34), 10335-10341• DOI: 10.1021/ja020565q • Publication Date (Web): 02 August 2003

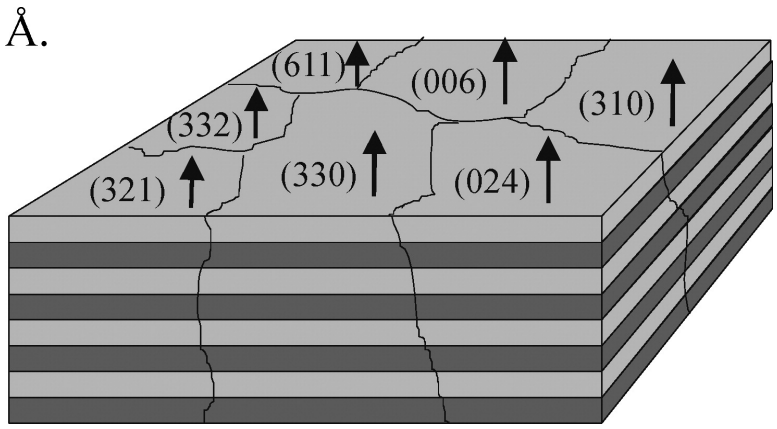

More About This Article

Additional resources and features associated with this article are available within the HTML version:

- Supporting Information
- Links to the 1 articles that cite this article, as of the time of this article download
- Access to high resolution figures
- Links to articles and content related to this article
- Copyright permission to reproduce figures and/or text from this article

View the Full Text HTML

J|A|C|S
ARTICLES
Published on Web 08/02/2003

Synthesis of Crystalline Skutterudite Superlattices Using the Modulated Elemental Reactant Method

Joshua R. Williams, Arwyn L. E. Smalley, Heike Sellinschegg, Carrie Daniels-Hafer, Jennifer Harris, Mark B. Johnson, and David C. Johnson*

Contribution from the Department of Chemistry and Material Science Institute, University of Oregon, Eugene, Oregon 97403

Received April 22, 2002; E-mail: davej@oregon.uoregon.edu

Abstract: A series of samples $((AB)_x(CD)_y)_z$ were prepared containing both short repeat units (AB and CD) and long repeat units $((AB)_x(CD)_y)$, where the short repeat units were designed to have the composition appropriate to form $\square M_4Sb_{12}$ skutterudites (M = Fe, Co, or Ir; $\square$ = vacancy, La, or Y). X-ray diffraction and reflectivity were used to follow the evolution of the films from amorphous, layered materials to crystalline skutterudite superlattices as a function of annealing temperature and time. In all cases, the short repeat units interdiffused and crystallized the expected skutterudite, while the long repeat period persisted after annealing. The skutterudites crystallize with random crystallographic orientation with respect to the substrate. The observed splitting of the peaks in the high-angle diffraction data from the $IrSb_3/CoSb_3$ sample indicates the formation of a novel superlattice structure with each grain having a random crystallographic orientation of the skutterudite lattice with respect to the superlattice direction.

Introduction

Recent discoveries and advances in the area of nanotechnology have attracted interest in the possible advantages of nanostructured and artificially structured materials. The possibility of producing new materials with "customized" properties by preparing structures that incorporate multiple materials has potential application in a number of areas, including laser diodes,[1] thermoelectrics,[2] and magnetic materials.[3,4] In the field of thermoelectrics, recent advances in the preparation of superlattice structures have led to significant increases in efficiency.[2]

Synthetically modulated structures have proven difficult to prepare using any traditional solid-state synthesis technique, presumably due to the lack of control over diffusion processes. A variety of layer-by-layer film growth techniques including molecular beam epitaxy, sputtering, chemical vapor deposition, and laser ablation deposition have been used to successfully produce new modulated structures.[5] All of these techniques produce crystalline superlattices using epitaxial growth, in which each layer is grown with a specific crystallographic relationship to the preceding layer. Epitaxial growth results from the manipulation of the substrate temperature and deposition rates to permit enough time and energy for each atom to find and occupy a lattice position within the growing crystalline surface. Extremely high-quality materials and atomically flat surfaces can be grown in this manner.[6−8]

It has recently been shown that superlattice structures can also be prepared through another method.[9] In this study, alternating groups of Nb−Se and Ti−Se bilayers were deposited on a cold substrate. Annealing led to interfacial nucleation and growth. When the annealing temperature and time were controlled, the samples formed crystalline superlattices aligned to the substrate. By accurately controlling the deposited layer thicknesses, we could control the number of unit cells of each phase in each superlattice period. As with the layer-by-layer growth techniques mentioned above, the superlattices prepared in this way were oriented in only one crystallographic direction.

We have used the modulated elemental reactant synthesis technique to prepare a wide variety of phases with the skutterudite crystal structure.[10−14] This synthesis method involves sequentially depositing ultrathin elemental layers to minimize the diffusion distance. This allows solid-state reactions to take place at very low temperatures (below 250° for the skutterudites) due to the small diffusion distances required for the reactants to form homogeneous and amorphous intermediates. Because the skutterudite crystal structure is cubic, and

(1) Peter, M.; Kiefer, R.; Fuchs, F.; Herres, N.; Winkler, K.; Bachem, K. H.; Wagner, J. *Appl. Phys. Lett.* **1999**, *74*, 1951−54.
(2) Venkatasubramanian, R.; Silvola, E.; Colpitts, T.; O'Quinn, B. *Nature* **2001**, *413*, 597−602.
(3) Kwo, J. R.; Gyorgy, E. M.; McWhan, D. B.; Hong, M.; DiSalvo, F. J.; Vettier, C.; Bower, J. E. *Phys. Rev. Lett.* **1985**, *55*, 397.
(4) Prinz, G. A.; Krebs, J. J. *Appl. Phys. Lett.* **1981**, *39*, 397.
(5) Solid State Sciences Committee. *National Research Council Report on Artificially Structured Materials*; National Academy Press: Washington, DC, 1985.
(6) Cho, A. Y. *Appl. Phys. Lett.* **1971**, *19*, 467.
(7) Cho, A. Y. *J. Appl. Phys.* **1971**, *42*, 2074.
(8) Cho, A. Y. *J. Appl. Phys.* **1970**, *41*, 2780.
(9) Noh, M.; Johnson, D. C. *J. Am. Chem. Soc.* **1996**, *118*, 9117−9122.
(10) Hornbostel, M. D.; Hyer, E. J.; Thiel, J.; Johnson, D. C. *J. Am. Chem. Soc.* **1997**, *119*, 2665−2669.
(11) Sellinschegg, H.; Stuckmeyer, S. L.; Hornbostel, M. D.; Johnson, D. C. *Chem. Mater.* **1998**, *10*, 1096−1101.
(12) Sellinschegg, H.; Williams, J. R.; Maxwell, S. P.; Sillars, D.; Johnson, D. C. *Mater. Res. Soc. Symp. Proc.* **1999**, *545*, 53−58.
(13) Sellinschegg, H.; Johnson, D. C.; Nolas, G. S.; Tritt, T. M. *Proc. Int. Conf. Thermoelectr.* **1999**, *18*, 19−22.
(14) Sellinschegg, H.; Smalley, A.; Yoon, G.; Johnson, D. C.; Nolas, G. S.; Kaeser, M.; Tritt, T. M. *Proc. Int. Conf. Thermoelectr.* **1999**, *18*, 352−355.

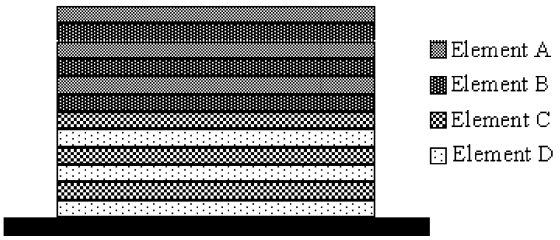

Figure 1. This drawing shows a representative elemental layering sequence for an individual period of the modulated elemental reactants prepared in this work. This period is repeated multiple times to build the initial reactant.

nucleates and grows from an amorphous intermediate, these phases crystallize with random orientation. Two new binary, and several new ternary "filled" skutterudite compounds with atoms occupying the large void in the center of the unit cell, have been prepared in this way.[10,12−15]

On the basis of the low nucleation and growth temperatures of these new skutterudite compounds from the amorphous intermediates, we wondered what would happen if we deposited elemental layers in a pattern such as that shown in Figure 1. Our thought was that, on low-temperature annealing, the layers would interdiffuse on the length scale of the elemental layering (A with B and C with D), without significant diffusion between the regions of different composition (AB vs CD). The extent of interdiffusion between the AB and CD layers would depend on the difference in the chemical potential between the layered structure and the mixed structure, the annealing temperature, and the length of time the sample was held at the annealing temperature. The chemical potential difference between an AB/CD layered compound and an ABCD mixture depends on both the enthalpy and the entropy of mixing of the components, with the enthalpy dependent on chemical similarities and differences between the layers. As we have observed in prior skutterudite studies, we would expect nucleation and growth of randomly oriented grains through the entire film thickness.[10,12,15] This is a fundamentally different growth mechanism than that used by the layer-by-layer epitaxial growth techniques, which involves controlling a surface "equilibrium" growth process. The final product should contain superlattice grains, where each grain would reflect the crystallographic orientation of the nucleation event.

To explore these ideas, we prepared three multilayered structures, each with a different pair of skutterudite phases. The three structures prepared were $FeSb_3/CoSb_3$, $La_xCo_4Sb_{12}/Y_xCo_4Sb_{12}$, and $IrSb_3/CoSb_3$. For the $FeSb_3/CoSb_3$ combination, there is a difference in lattice parameter (9.18 Å/9.04 Å) between the binary compounds, and the difference in electron count between these two compounds might result in a significant enthalpic driving force for intermixing. For the $La_xCo_4Sb_{12}/Y_xCo_4Sb_{12}$ combination, there is essentially no lattice parameter difference (9.08 Å/9.07 Å), and we expect the chemical similarity of the lanthanide elements and the fact that they occupy the same position in both compounds would result in only a small enthalpic driving force for intermixing. For the $IrSb_3/CoSb_3$ combination, there is a larger difference in lattice parameter (9.24 Å/9.04 Å), and again we expect no significant enthalpic driving force for intermixing as they are isoelectronic and both Ir and Co occupy equivalent crystallographic sites in the component crystals.

Experimental Section

All samples were prepared by evaporative deposition onto a silicon substrate coated with polymethyl methacrylate (PMMA) for easy sample removal. Additionally, miscut quartz and polished silicon pieces were affixed to the substrate for later use in X-ray diffraction and reflectivity experiments. Thermionics electron beam guns were used, at a rate of 0.5 Å/s, to deposit all elements other than Sb. Antimony was deposited from a custom-built Knudsen cell at a rate of 0.8 Å/s. The background pressure in the deposition chamber was maintained at 10^{-6} Torr or better during the entire deposition. The deposition sequence was controlled by a personal computer running custom-authored automation software. Deposition rates and thicknesses for each deposition source were monitored using Leybold-Inficon XTC and XTC/2 quartz crystal thickness monitors.

The sample was released from the PMMA-coated silicon substrate by soaking the substrate in acetone to dissolve the PMMA layer. After the sample is lifted off the substrate surface, it is collected by vacuum filtration using Teflon filter paper.

X-ray diffraction and reflectivity experiments on coated pieces (either miscut quartz or polished silicon) were performed on a Phillips MRD 4-circle system. X-ray diffraction of sample pieces after differential scanning calorimetry was performed on a Scintag XDS 2000 diffractometer. All X-ray experiments were performed using Cu Kα radiation.

Differential scanning calorimetry was performed on sample pieces after release from the silicon substrate. Approximately one-half of a milligram of sample was placed and sealed in an Al sample pan and was heated at a programmed rate, while the heat flow in and out of the sample was monitored. This heat flow was compared to an empty reference pan of identical type. The difference in the heat flow between the two pans is assumed to be attributable to the sample contained in the sample pan.

Sample composition was measured by electron probe microanalysis (EPMA) using a Cameca S-50 instrument with a 10 kV accelerating voltage, 10 nA beam current, 1 μm spot size, and an energy dispersive detector.

Results

$FeSb_3/CoSb_3$. The elementally modulated $FeSb_3/CoSb_3$ reactant consisted of 7 Fe/Sb bilayers followed by 7 Co/Sb bilayers to construct one period. The intended thickness of each bilayer was 15 Å. The total film structure consisted of 9 periods, each intended to be 210 Å thick, with a total intended film thickness of 1890 Å. The actual period thickness and total film thickness, as measured by X-ray diffraction, were 215 (±5) and 1940 (±20) Å, respectively. The composition of the film was determined by EPMA to be $Co_{1.5}Fe_{2.6}Sb_{12}$.

To understand the reactivity of this multilayer, differential scanning calorimetry (DSC) was performed to measure the temperature at which significant thermal events occurred during annealing. Typically the DSC data for skutterudite phases prepared using the modulated elemental reactant method consist of a single sharp exotherm caused by nucleation and growth of the crystalline phase from the amorphous intermediate.[10,11] When prepared individually, $CoSb_3$ typically nucleates around 175 °C, while $FeSb_3$ nucleates around 150 °C.[10] Interestingly, the DSC data for this multilayer contained just a single sharp exotherm at 160 °C − right between the exotherm temperatures typically observed for each phase individually. To determine the cause of this, and to understand how the layered structure might change with annealing, X-ray reflectivity and diffraction studies

(15) Williams, J. R.; Johnson, D. C. *Inorg. Chem.* **2002**, *41*, 4127−4130.

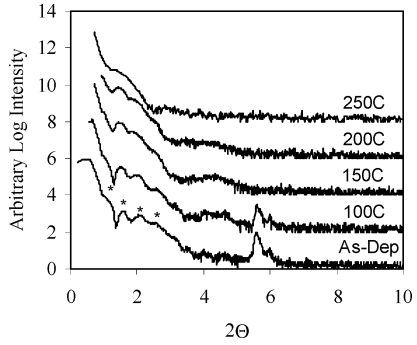

Figure 2. X-ray reflectivity data collected at various annealing temperatures showing peaks corresponding to the period spacing (*) as well as a Bragg peak at ~5.6° 2θ which arises due to the fact that a large amount of this Fourier component is needed to describe the elemental layering of the sample. The sample was annealed for 1 h at the indicated temperatures.

were performed after annealing the sample at various temperatures. An X-ray reflectivity study of the sample after various annealing steps is shown in Figure 2.

There are two key features of these data that should be noted, and which are most easily recognized by examining the as-deposited data. The data contain low-intensity periodic peaks (marked with *) that correspond to the 215 (±5) Å period spacing of the multilayer as well as the higher intensity Bragg peak observed at ~5.7°. This peak has higher intensity because more of this Fourier component is needed to describe the layered structure, because the *d* spacing corresponding to this peak is close to the thicknesses of the Fe−Sb and Co−Sb bilayers used to build up the repeating unit. Note that the intensity of this Bragg peak diminishes with annealing, and it disappears entirely after annealing at 150 °C. Consequently, this Fourier component is no longer necessary to describe the electron density profile of the sample, indicating that the Fe/Sb and Co/Sb layering of the sample is no longer intact. The peaks from the period spacing of the multilayer are still observed and not significantly changed at this temperature, indicating that the sample is still layered on the 215 Å length scale. These periodic maxima disappear after annealing the sample at 250 °C, indicating that at this temperature the sample no longer has a defined layered structure. This suggests that the regions of different composition have interdiffused.

The high-angle X-ray diffraction data for this system show the conversion of a previously X-ray amorphous material to one with the crystalline skutterudite structure, after being annealed at 150 °C. The skutterudite has a lattice size of 9.12-(1) Å, which is between the previously measured values for $FeSb_3$ and $CoSb_3$.[10,11] This is also the annealing temperature where the elemental layering is observed to disappear in the X-ray reflectivity data. This diffraction data lacked high-frequency maxima indicative of superlattice formation. These maxima can be quite intense in superlattices composed of highly oriented materials.[9] The random orientation of the skutterudite phase should produce lower intensity versions of these maxima. The lack of these maxima in the diffraction data is attributable to three possible causes. The first is that, rather than forming an $FeSb_3/CoSb_3$ superlattice structure, the sample actually consists of a mixture of an $Co_{1-x}Fe_xSb_3$ alloy and a region that remains layered. The second is that the grain size of the crystalline superlattice perpendicular to substrate is small due to multiple nucleation events leading to multiple crystallites with different orientations. The line widths of the diffraction maxima suggest that the grain sizes perpendicular to the substrate are on the order of the multilayer period thickness. The third is that the small difference in the scattering power between the Fe and Co in $FeSb_3$ and $CoSb_3$ results in unobservable weak superlattice peaks. The latter seems the more likely explanation, as the reflectivity data clearly indicated that the sample is still layered on the length scale of the period up to an annealing temperature of 200 °C − well after the nucleation of the skutterudite phase.

$La_xCo_4Sb_{12}/Y_yCo_4Sb_{12}$. In an attempt to create a multilayer of "filled" skutterudite materials, a multilayer was constructed consisting of alternating La/Co/Sb and Y/Co/Sb trilayers. The intended thickness of each trilayer was 17 Å, and the repeat period was intended to be 34 Å, consisting of one set of each trilayer. The total film structure consisted of 22 periods, for a total intended film thickness of 748 Å. The actual measured period thickness and total film thickness were 27 (±1) and 610 (±5) Å, respectively. EPMA of this sample showed the composition to be $La_{0.4}Y_{0.7}Co_{3.5}Sb_{12}$.

As in the Fe−Sb/Co−Sb case, we again see a single exothermic peak at 227 °C in the DSC data, which is close to the temperatures where previous La/Co/Sb[13] and Y/Co/Sb reactants were separately observed to nucleate and grow. The X-ray reflectivity pattern of this multilayer stack contains a Bragg peak from the Fourier component close to that of the repeat trilayer spacing (at ~5.8° 2θ) and a first-order Bragg peak corresponding to the period of the multilayer (at ~3.3° 2θ).

Shown in Figure 3 is the X-ray diffraction pattern of this sample as deposited and at various annealing temperatures. Note that the sample is amorphous with respect to X-ray diffraction until it is annealed at 200 °C. At this temperature, the X-ray reflectivity data show that the peak corresponding to the repeat unit layering is no longer visible, but the peak corresponding to the period of the layering (at 3.2° 2θ) is still observed. This again indicates that after nucleation of the skutterudite phase the elemental layering of the sample is no longer intact, but the periodic repeat of two trilayers remains. As in the Fe−Sb/Co−Sb case above, there is no evidence of satellite peaks resulting from the superlattice layering in the high-angle diffraction data. Similarly, this is likely due to the minimal electron density contrast between the two phases and the fact that skutterudites nucleate in a randomly oriented fashion. As with the previous sample, the line width of the diffraction peaks is consistent with the grain size being comparable to the film thickness, suggesting that, once nucleated, grain growth is rapid. Note that, as compared to the Fe−Sb/Co−Sb case, higher temperatures (>250 °C) and longer times are required to eliminate the maxima due to the repeating structure of the sample.

This higher temperature stability of the "filled" skutterudite superlattice as compared to the "unfilled" $FeSb_3/CoSb_3$ sample above is potentially attributable to two key differences between these structures. The first key difference is the filling of the void in the center of the skutterudite unit cell. In one case, this void is filled with either La or Y, and in the other case it remains unfilled. This unfilled void in the $FeSb_3/CoSb_3$ superlattice could potentially provide a diffusion pathway not found in the filled superlattice. The void is certainly large enough to accommodate an atom of any of the elements in these samples, and it has

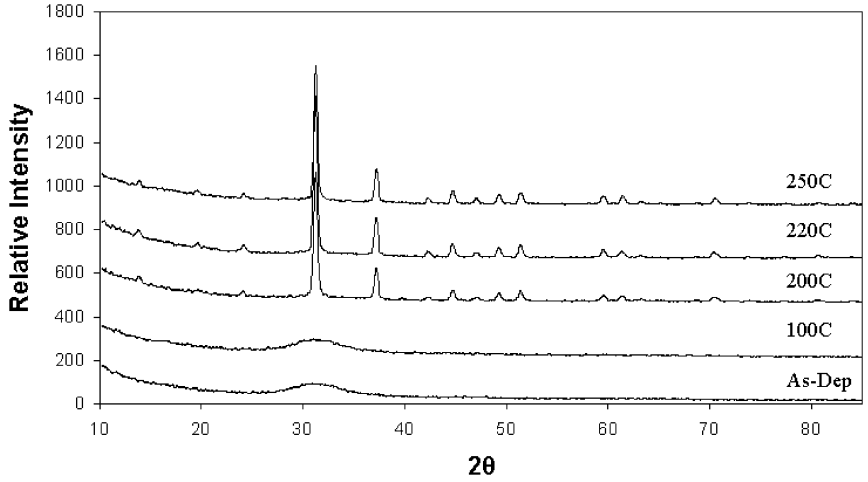

Figure 3. X-ray diffraction data showing the nucleation of the skutterudite phase from a previously X-ray amorphous material after annealing to 200 °C. No satellite peaks characteristic of superlattice structure are observed.

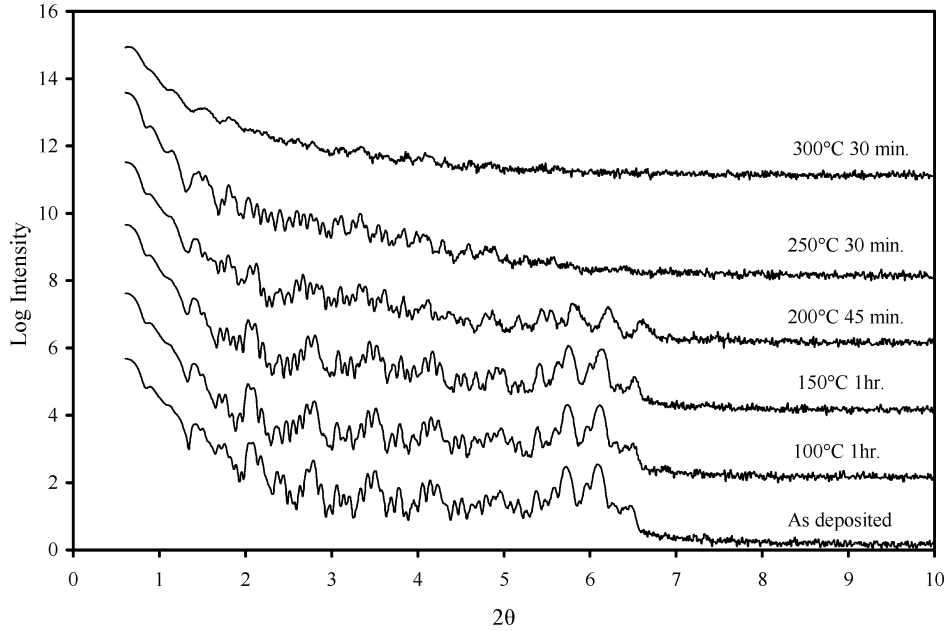

Figure 4. X-ray reflectivity data from a film on a silicon substrate showing how the layering of the superlattice sample changes with annealing temperature and time. The small, high-frequency peaks are Kiessig fringes and are due to the total sample thickness; the larger peaks are due to the superlattice repeat thickness of ~225 Å.

been shown that atoms occupying this void are in a very loosely bound state.[16] Another key distinction is the difference in electron count between $FeSb_3$ and $CoSb_3$ in the unfilled case, which may provide a stronger driving force for interdiffusion than that in the filled isoelectronic pair, $La_xCo_4Sb_{12}$ and Y_x-Co_4Sb_{12}.

$IrSb_3$/$CoSb_3$. The Ir−Sb/Co−Sb structure, consisting of alternating Ir/Sb and Co/Sb bilayers, was chosen because the scattering power contrast between these two phases is greater than in either of the two other samples, increasing the likelihood that maxima in the high-angle diffraction pattern expected from a superlattice structure would be experimentally observed. The intended thickness of each bilayer was 15 Å. Seven bilayers of each type were alternated to produce a period with a total of 14 bilayers. The intended thickness of this period was 210 Å, and with a total of 8 periods deposited the total intended film thickness was 1680 Å. The actual period thickness and total film thickness were 225 (±5) and 1760 (±10) Å, respectively. Microprobe analysis of this sample showed the composition to be $Ir_{2.4}Co_{2.4}Sb_{12}$.

X-ray reflectivity data collected on the film as deposited and at a variety of annealing conditions are shown in Figure 4. The periodic maxima arising from the period spacing of the multilayer can be clearly seen (marked with *), with several diffraction orders around 6° 2θ being more intense as a result of the 15 Å repeat unit in the structure. On annealing, the intensity of these maxima slowly decreases as the elements interdiffuse on the length scale of the repeat unit. The number of diffraction orders does not decrease, suggesting that the regions of different composition (Ir−Sb vs Co−Sb) remain segregated and the interface between them does not significantly broaden. Also note that the positions of the peaks shift to higher 2θ angles after the 200 °C annealings, indicating a contraction in the repeat unit. Annealing at 250 °C results in the disap-

(16) Sales, B.; Chakoumakos, B.; Mandrus, D.; Sharp, J. *J. Solid State Chem.* **1999**, *146*, 528−532.

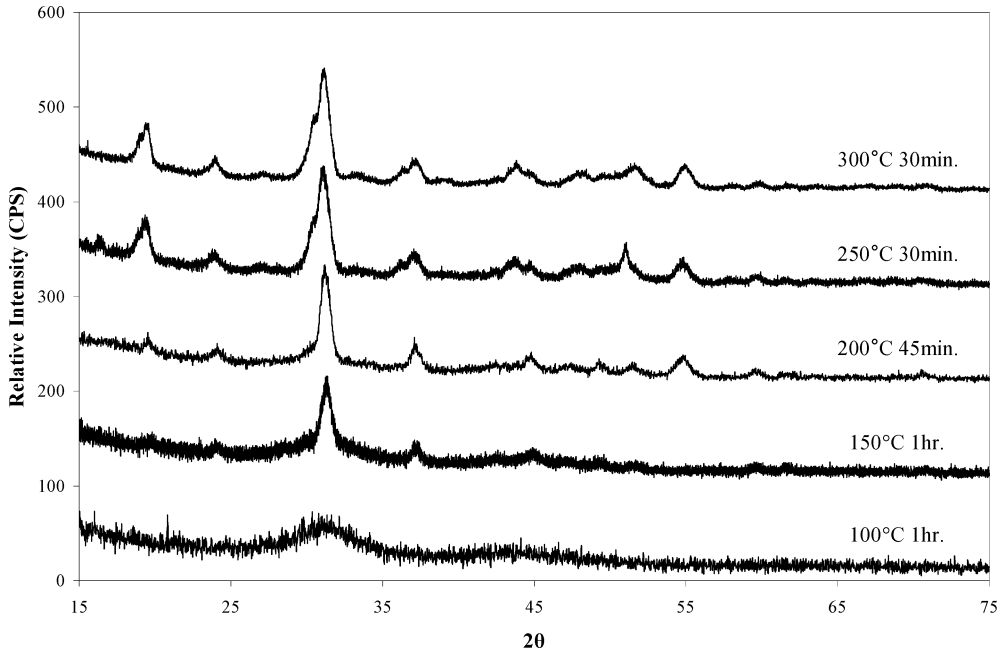

Figure 5. X-ray diffraction data collected from sample film deposited on a zero-background quartz piece.

pearance of the peaks at ~6° 2θ, indicating the interdiffusion on the length scale of the elemental layering (A with B and C with D). The earlier loss of the high-frequency Kiessig fringes on scanning from low to high angles in the 250 °C scan also implies that the sample roughness has increased. At 300 °C, one can still see diffraction maxima from the ~225 Å repeat, but further loss of the Kiessig fringes indicates additional sample roughness.

The X-ray diffraction data shown in Figure 5 were collected from a thin-film sample deposited directly onto a piece of miscut quartz, a material commonly used as a zero-background substrate for X-ray diffraction experiments. The skutterudite diffraction pattern begins to be visible after annealing the sample at 150 °C for 30 min. The lattice parameter refined from this pattern matches that expected for $CoSb_3$. Annealing to 200 °C results in an unknown phase growing in, contributing a diffraction peak at ~55° 2θ. After annealing at 200 °C for 45 min, a shoulder appears on the low-angle side of the $CoSb_3$ peak at ~31° 2θ, at the position expected for $IrSb_3$. At 250 °C, the diffraction patterns of both skutterudite phases are easily visible. As with the previous two systems discussed, these X-ray data lack the high-frequency maxima that would confirm that superlattice formation had occurred. The large peak widths indicate that the crystallites perpendicular to the substrate in this thin film sample are very small, ~100 Å. These crystallites are one-half the size of those observed in the $FeSb_3/CoSb_3$ and $LaCo_4Sb_{12}/YCo_4Sb_{12}$ samples discussed previously.

DSC analysis for powdered samples, shown in Figure 6, showed results strikingly different from the single, sharp exotherm that is usually observed for skutterudite samples. These DSC results were also observed for the other two systems in this study. This multiple-peak pattern was observed for several Ir−Sb/Co−Sb samples prepared with a variety of different layering periods. To investigate the cause of the additional peaks, we conducted an X-ray diffraction study of the powders annealed to each of the temperatures indicated by arrows in Figure 6 (see Figure 7).

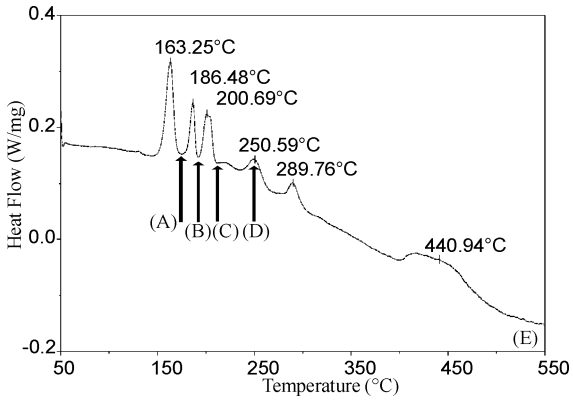

Figure 6. Differential scanning calorimetry data from a powdered sample showing multiple exothermic events.

X-ray diffraction data collected from a powdered sample annealed to the temperatures indicated in Figure 6 provide insight into the structural changes associated with the exotherms observed in the DSC data. After the first exotherm (165 °C), the sample has crystalline $CoSb_3$ present. After the second exotherm (185 °C), the same unknown phase observed in the film sample has appeared, with a diffraction maximum at ~55° 2θ. After the third exotherm (200 °C), $IrSb_3$ has formed, as indicated by the low-angle shoulders on the $CoSb_3$ peaks. After annealing to 250 °C, crystallite size increased, but it was still too small to give sufficient resolution to determine whether a superlattice phase was present.

Diffraction data after annealing to 550 °C provided strong evidence that a superlattice formed. In addition to further increases in crystallite size, subsidiary maxima were clearly visible on the peaks centered at 31° and 44° 2θ. Figure 8 contains an expanded view of the peak at 31° 2θ for both the C and the E scans of Figure 7. In addition to the appearance of the subsidiary maxima, there is also a significant shift in the location of the highest intensity in this peak from its former location at C. This position no longer corresponds to the expected locations of either the $IrSb_3$ or the $CoSb_3$ (310)

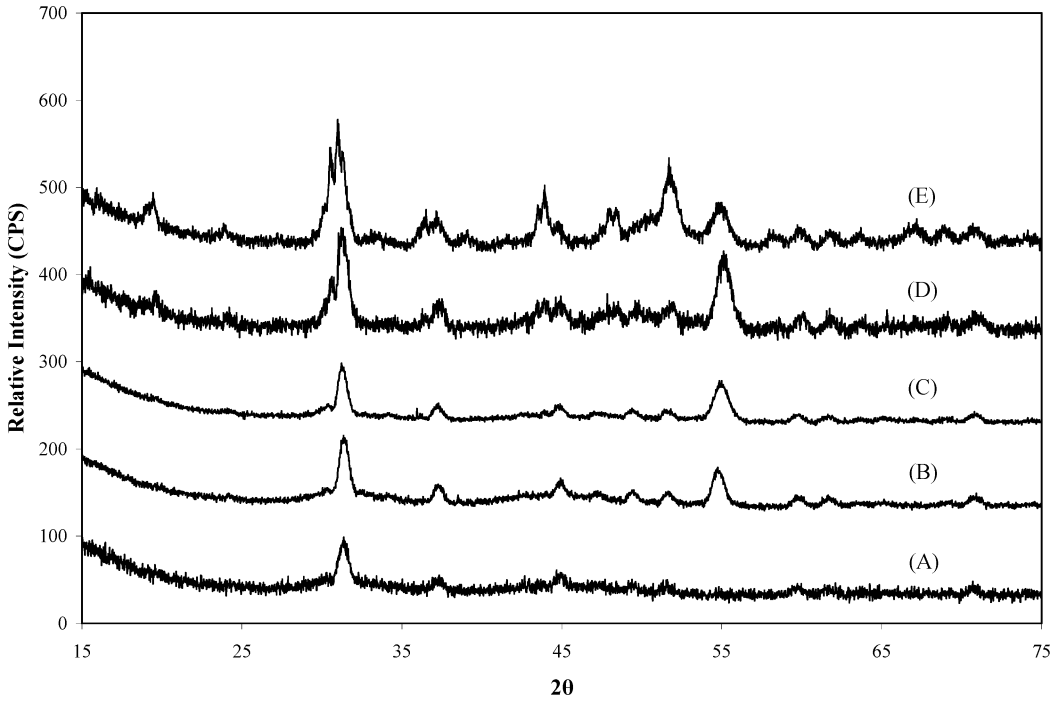

Figure 7. X-ray diffraction data collected from powder after differential scanning calorimetry. The data labels correspond to arrows in the DSC data shown in Figure 6, indicating the temperature at which the sample was removed from the DSC for X-ray analysis.

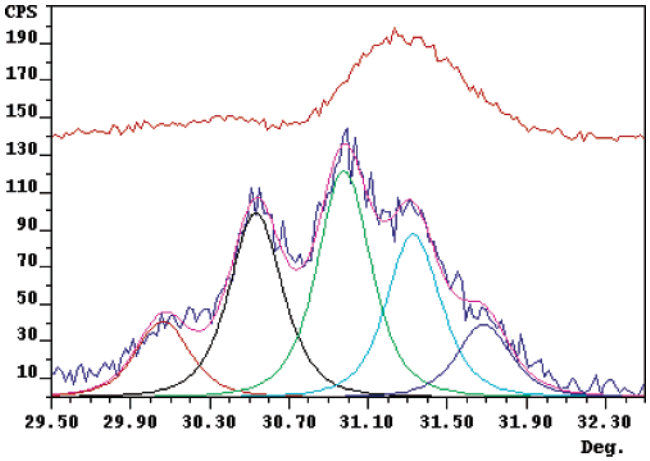

Figure 8. Display of peak fitting used to determine the position of the satellite peaks for analysis as shown in eq 1. The ±1 and ±2 superlattice peaks are visible in addition to the main (310) peak. Similar fitting was performed on the satellites around the (024) peak, giving the position of the ±1 peaks only. This analysis is performed on sample E from Figure 7. Scan C is above in red, showing the shift in the position of the peak maximum.

diffraction maxima. This structural change can be linked to the additional exothermic peaks visible in Figure 6 between 250 and 550 °C.

The period of the superlattice can be extracted from the positions of the satellite peaks on each side of the peaks centered at 31° and 44° 2θ as demonstrated by Lashmore and Dariel.[17] The modulation wavelength Λ can be calculated from the position of the satellite peaks using eq 1 below:

$$\Lambda_x = \frac{n\lambda}{\sin\theta_+ - \sin\theta_-} \qquad (1)$$

θ_+ and θ_- are the positions of the higher-angle (+) and lower-angle (−) satellite peaks, respectively. The order of the satellite peaks is represented by n, and the X-ray wavelength is represented by λ. The superlattice period value extracted (see Table 1) is consistent for both peaks and matches the 225 (±5) Å period of the initial layered structure (shown by X-ray reflectivity). These data confirm formation of a superlattice.

Table 1. Peak Positions Derived from Peak-Fitting of the Satellite and Main Peaks around the Positions Expected for the (310) and (024) Reflections of the $CoSb_3$ and $IrSb_3$ Skutterudites[a]

Miller indices	2θ peak position (−2)	2θ peak position (−1)	2θ peak position (0)	2θ peak position (+1)	2θ peak position (+2)	Λ_x from ±1	Λ_x from ±2
(310)	30.05	30.52	30.96	31.31	31.67	230 Å	230 Å
(024)	n.a.	43.48	43.91	44.31	n.a.	230 Å	n.a.

[a] Thickness values for the superlattice structure causing these satellite peaks are computed using eq 1. The average value for the superlattice period is 230 ± 10 Å.

In addition to being a superlattice, the diffraction data in scan E suggest that this sample is randomly oriented. Note that in scan E the sample continues to show intensity maxima in all of the regions it previously had, when the sample showed only $CoSb_3$ and $IrSb_3$. If the sample had preferential orientation, we would expect to see a set of satellite peaks centered at the position expected for the reflection corresponding to the preferred orientation, and nowhere else. Because we continue to see intensity maxima at all of the positions expected for a randomly oriented sample, this sample consists of randomly oriented superlattice crystallites. A model of this proposed structure can be found in Figure 9. Because the sample is made of randomly oriented crystallite, we analyzed the diffraction data according to the method of Lashmore and Dariel, which treats each set of satellites independently.

This structure is quite different from epitaxially grown superlattices that are more commonly reported. For superlattice

(17) Lashmore, D. S.; Dariel, M. P. *J. Electrochem. Soc.* **1988**, *135*, 1218−1221

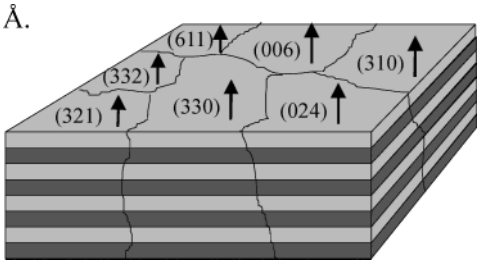

Figure 9. A possible representation of the randomized superlattice structure. Although these grains are shown as being the full film thickness, in actuality they are ~400 Å, significantly smaller than the total film thickness.

applications that rely on having highly oriented structures, this type of randomized superlattice arrangement would most likely be a detriment rather than an advantage. For other applications, however, this unusual type of structure could be very desirable. For example, recent work on preparing new materials designed for high thermoelectric efficiency has shown that superlattice structures can provide a marked decrease in the lattice thermal conductivity of the constituent materials without significantly affecting their electrical transport properties.[2] The randomized superlattice structure presented here could have even lower lattice thermal conductivity due to scattering of phonons at the superlattice grain interfaces. Characterization of this kind of structure will present challenges, as the properties may change considerably from grain to grain as a result of the different relative crystallographic orientation of the skutterudite structure in the superlattice.

Summary

The evolution of three modulated elemental reactants into superlattice structures was followed through annealing using both high- and low-angle X-ray diffraction. The data presented suggest that three skutterudite superlattice structures composed of different combinations of skutterudite phases have been synthesized. Diffraction data in the powdered sample of the $IrSb_3/CoSb_3$ case indicate that, for the first time, a randomly oriented superlattice has been synthesized.

Acknowledgment. This material is based upon work supported by the National Science Foundation under Grant No. DMR0103409. In addition, one of us (JW) is grateful for support from the IGERT Fellowship under Grant No. DGE0114419, and one of us (AS) is grateful for support from the GAANN Fellowship under Grant No. P200A80234.

JA020565Q